

# Mathematical Micro-Model of a Solid Oxide Fuel Cell Composite Cathode

Ben Kenney, Kunal Karan

Fuel Cell Research Centre, Department of Chemical Engineering  
Queen's University, Kingston, ON, Canada

## **Abstract**

In a solid oxide fuel cell (SOFC), the cathode processes account for a majority of the overall electrochemical losses. A composite cathode comprising a mixture of ion-conducting electrolyte and electron-conducting electro-catalyst can help minimize cathode losses provided microstructural parameters such as particle-size, composition, and porosity are optimized. The cost of composite cathode research can be greatly reduced by incorporating mathematical models into the development cycle. Incorporated with reliable experimental data, it is possible to conduct a parametric study using a model and the predicted results can be used as guides for component design. Many electrode models treat the cathode process simplistically by considering only the charge-transfer reaction for low overpotentials or the gas-diffusion at high overpotentials. Further, in these models an average property of the cathode internal microstructure is assumed.

This paper will outline the development of a 1-dimensional SOFC composite cathode micro-model and the experimental procedures for obtaining accurate parameter estimates. The micro-model considers the details of the cathode microstructure such as porosity, composition and particle-size of the ionic and electronic phases, and their interrelationship to the charge-transfer reaction and mass transport processes. The micro-model will be validated against experimental data to determine its usefulness for performance prediction.

## **1 Introduction**

Mathematical models are important tools for the research and development cycle and are being used to accelerate commercialization of solid oxide fuel cells (SOFC). A model is only a useful predictive tool if it can incorporate as many physical, chemical and electrochemical processes as possible and if it includes accurate experimental parameters. Models available in the literature however don't generally include all of these fundamental processes and use outdated or inaccurate experimental parameters.

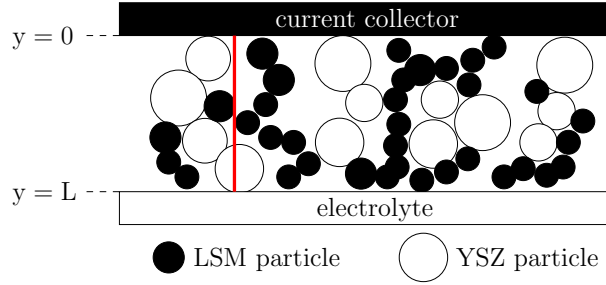


Figure 1: 1-dimensional computational domain.

The state-of-the-art SOFC anode is a Ni/YSZ composite cermet, and the LSM/YSZ composite cathode is known to greatly improve cathode performance. Although the presence of electrolyte material in the cathode decreases the electrical conductivity, the performance enhancement is a result of greatly increased active area. These electrodes cannot be modelled as a thin reactive boundary since this method does not capture the local current densities or local overpotentials throughout the thickness. Despite this fact, only a small number of researchers have modelled composite electrodes [1, 2, 3, 4, 5] and use experimental parameters such as exchange current densities from other labs. Since experimental parameters depend on fabrication technique and testing method, there exists a wide variation of parameters in the literature which makes model validation difficult.

The model presented here is a 1-dimensional LSM/YSZ composite cathode and is accompanied with experimental data that is used for the electrochemical parameters and also for validation of the model.

## 2 Model Development

### 2.1 Model Domain

A 1-dimensional isothermal composite cathode model was developed. This model includes parameters such as LSM and YSZ composition, particle size, porosity and thickness. The model also incorporates percolation thresholds for the LSM phase and YSZ phase which significantly influences the conductivity. Figure 1 shows the computational domain which consists of random packed spheres that represent LSM and YSZ particles.

### 2.2 Charge Transport

The governing equations for charge transport are Ohm's Law for both the electronic and ionic conducting species and a charge balance. We can write a balance on the electronic current and ionic current as:

$$\lambda_{TPBL} \times [i_{anodic} - i_{cathodic}] = -\frac{\partial}{\partial x}(i_{el}) = \frac{\partial}{\partial x}(i_{io}) \quad (1)$$

where  $el$  and  $io$  are electronic and ionic conducting phases,  $i$  is the current density (A/m<sup>2</sup>),  $\lambda_{TPBL}$  is the triple phase boundary line length per geometric volume (m/m<sup>3</sup>),  $i_{anodic}$  and  $i_{cathodic}$  are associated with the Butler-Volmer equation. Inserting Ohm's Law into the charge balance (Equation 1),

$$\lambda_{TPBL} \times [i_{anodic} - i_{cathodic}] = -\frac{\partial}{\partial x}(\sigma_{el}^{eff} \nabla \phi_{el}) = \frac{\partial}{\partial x}(\sigma_{io}^{eff} \nabla \phi_{io}) \quad (2)$$

where  $\sigma^{eff}$  is the effective conductivity of the electronic or ionic phase and  $\phi$  is the potential. We can now generalize to 3-dimensions and get the Laplacian charge balance

$$\lambda_{TPBL} \times [i_{anodic} - i_{cathodic}] = -\nabla \cdot (\sigma_{el}^{eff} \nabla \phi_{el}) = \nabla \cdot (\sigma_{io}^{eff} \nabla \phi_{io}) \quad (3)$$

The anodic and cathodic currents are described by the Butler-Volmer equation and can be written for a single rate determining step as,

$$i_{anodic} = i_{0,a} \exp(\alpha_a f \eta) \quad (4)$$

$$i_{cathodic} = i_{0,c} \exp(-\alpha_c f \eta) \quad (5)$$

where

$$\eta = (\phi_{io} - \phi_{el}) \quad (6)$$

and the local exchange current density can be written as

$$i_0 = i_0^{ref} \left( \frac{O_2}{O_2^{ref}} \right)^\gamma \quad (7)$$

## 2.3 Species Transport

Concentration overpotential should not be solved explicitly, it is implied when solving for the local exchange current density (Equation 7), since at very low  $O_2$  concentrations, the exchange current density is small. The Stefan-Maxwell equation was used to solve for local species concentration:

$$-\frac{M_{O_2} \lambda_{TPBL}}{4F} \times [i_{anodic} - i_{cathodic}] = \sum_{j=1, j \neq i}^n \frac{X_j N_i - X_i N_j}{c D_{i,j}} \quad (8)$$

and the binary diffusivity is calculated from

$$\frac{pD_{O_2-N_2}}{(p_{c,O_2}p_{c,N_2})^{1/3}(T_{c,O_2}T_{c,N_2})^{5/12}\left(\frac{1}{M_{O_2}} + \frac{1}{M_{N_2}}\right)} = A \left( \frac{T}{\sqrt{T_{c,O_2}T_{c,N_2}}} \right)^B \quad (9)$$

$$D_{O_2-N_2}^{eff} = \left( \frac{\tau}{\epsilon D_{O_2-N_2}} \right)^{-1} \quad (10)$$

where  $T_c$  and  $p_c$  are the critical temperatures and critical pressures,  $A$  is  $2.745 \times 10^{-6}$ ,  $B$  is 1.823 and  $\tau$  is the tortuosity (15.6 [6]).

## 2.4 Boundary Conditions

Some models [1, 2] assume that the electronic current is completely consumed at the cathode/electrolyte interface (ie:  $i_{el} = 0$  cathode/electrolyte interface). This however is not necessarily the case and better boundary conditions for the electronic current is a no flux condition, similar to the species balance boundary conditions at that interface. This boundary condition is a result of a dense, non-electronically conducting electrolyte.

$y=0$

$$\phi_{el} = 0, \mathbf{n} \cdot \mathbf{J}_{iO} = 0, w_{O_2} = 0.21 \quad (11)$$

$y=L$

$$\mathbf{n} \cdot \mathbf{J}_{eI} = 0, \phi_{iO} = \eta, \mathbf{n} \cdot \mathbf{N} = 0 \quad (12)$$

## 2.5 Model Parameters

*TPB line length:* An expression for the triple phase boundary line length per unit volume was developed by Sunde [2] using the relationship between percolation and particle coordination for binary power mixtures developed by Bouvard and Lange [7].

$$\lambda_{TPBL} = 2\pi r \sin \theta n n_{iO} n_{el} \frac{Z_{iO} Z_{el}}{Z} p_{iO} p_{el} \quad (13)$$

where  $\theta$  is the contact angle between LSM and YSZ particles ( $15^\circ$ ),  $n$  is the number of particles per unit volume,  $n_{el}$  and  $n_{iO}$  is the number fraction of particles,  $Z_{iO}$  and  $Z_{el}$  are the particle coordination numbers (the number of particles that are in direct contact with each other),  $Z$  is the average number of contacts for each particle (6) and  $p_{iO}$  and  $p_{el}$  are the probabilities of percolation for each conducting phase.

$$n = \frac{1 - \epsilon}{\frac{4}{3}\pi r_{el}^3 [n_{el} + (1 - n_{el})\left(\frac{r_{iO}}{r_{el}}\right)^3]} \quad (14)$$

where  $\epsilon$  is the porosity of the material and  $r_{el}$  and  $r_{io}$  is the radius of electronically and ionically conducting particles. The probability of percolation can be calculated from [7],

$$p_i = \left[ 1 - \left( \frac{4.236 - Z_{i-i}}{2} \right)^{2.5} \right]^{0.4} \quad (15)$$

$$Z_{i-i} = n_i \frac{Z_i^2}{Z} \quad (16)$$

$$Z_{io} = 3 + \frac{(Z - 3) \left( \frac{r_{io}}{r_{el}} \right)^2}{n_{el} + (1 - n_{el}) \left( \frac{r_{io}}{r_{el}} \right)^2} \quad (17)$$

$$Z_{el} = 3 + \frac{(Z - 3)}{n_{el} + (1 - n_{el}) \left( \frac{r_{io}}{r_{el}} \right)^2} \quad (18)$$

*Effective Resistivity:* The electrical resistivity (inverse of conductivity) of the pure material must be adjusted to an effective property in order to account for microstructural effects, such as porosity and composition which work to increase the resistivity. The following effective resistivity model has been used by Chen et al. [5] and is also used here,

$$\rho_j^{eff} = \frac{\rho_j^0}{(1 - \epsilon)\vartheta_j p_j} \quad (19)$$

where subscript  $j$  can be either  $el$  or  $io$ ,  $\rho^0$  is the resistivity of the pure material,  $\epsilon$  is the porosity of the electrode,  $\vartheta$  is the volume fraction and  $p$  is the probability of percolation which is a function of particle size. If the electrical network is non percolating, then the resistivity of the electrode increases by orders of magnitude [8] and is effectively non-conducting.

The conductivities of the pure material (in  $S/cm$ ) are [NexTech]:

$$\sigma_{LSM} = 0.244T - 8.412 \quad (20)$$

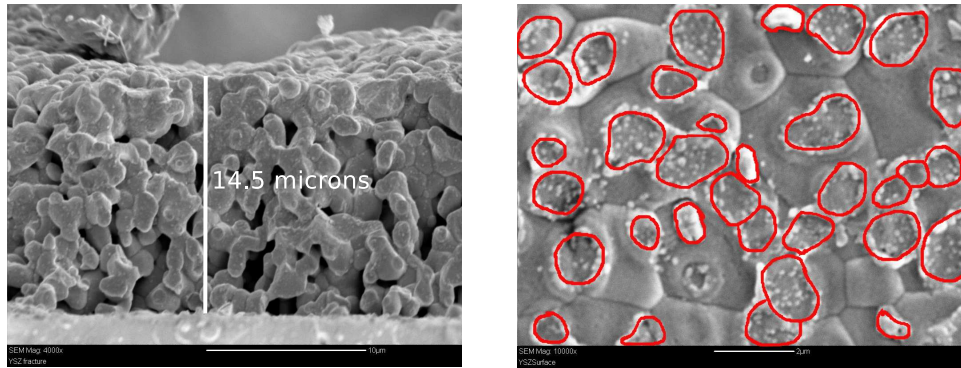
$$\ln \sigma_{YSZ} = 0.0127T - 17.463 \quad (21)$$

where  $T$  is temperature in  $K$ .

### 3 Electrochemical Characterization

Electrochemical parameters, exchange current density ( $i_0$ ), reaction order ( $\gamma$ ) and charge transfer coefficients ( $\alpha_a$ ,  $\alpha_c$ ) were determined experimentally using 3-electrode configuration where the cathode overpotential can be calculated from

$$\eta_{cathode} = V_{measured} - IR_{serial} \quad (22)$$



(a) Cross Section

(b) Fingerprint

Figure 2: SEM micrographs of LSM cross section and fingerprint region of 3-electrode cell

where  $V_{measured}$  is the potential measured between the reference electrode and the working electrode,  $R_{serial}$  is the resistance of the electrolyte, measured by impedance spectroscopy and  $I$  is the current.

### 3.1 Experimental

YSZ powder (Tosoh, USA) was dry pressed into dense 1.3mm disks and sintered at 1400°C for 5 hrs. LSM powder (NexTech, USA) was sprayed onto the YSZ electrolyte disk and sintered at 1200°C for 2 hrs. A Pt reference electrode and Pt counter electrode were applied to the electrolyte so that the ratio of the distance between the working and reference electrode to the disk thickness was larger than 5. Pt mesh was applied as the current collector to the working, reference and counter electrodes. I-V measurements were performed after applying a voltage of 0.4V for 1 hr in order to activate the cathode. Immediately after the I-V measurement, an impedance measurement was performed in order to extract the resistance of the electrolyte. This procedure was repeated for a 60 vol% LSM and 40 vol% YSZ composite working electrode. The surface of the working electrode was etched off and S.E.M. micrographs were obtained in order to view the cross-section and to estimate the TPB line length from the contact between LSM and YSZ electrolyte (Figures 2(a) and 2(b)). Figure 3 shows the I-V curves for the LSM working electrode sample and the extracted parameters from the data.

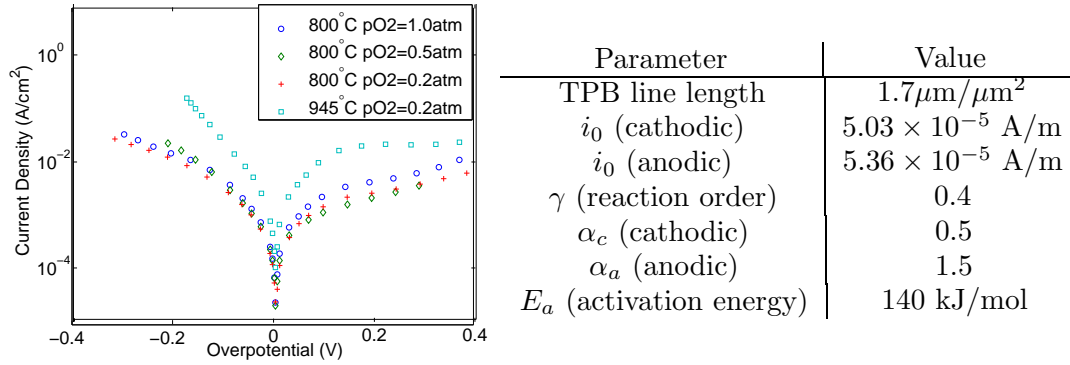


Figure 3: 3-electrode I-V measurements and resulting model parameters.

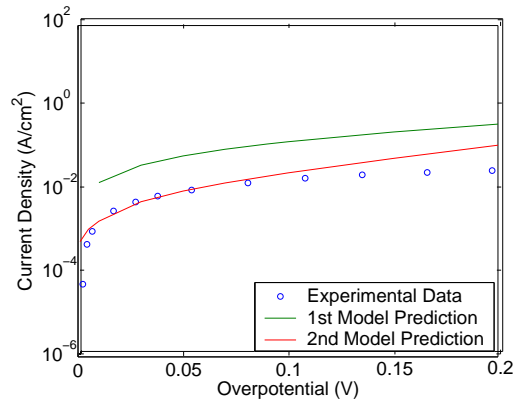


Figure 4: Comparison of simulation to experimental results for 60 vol% LSM, 40 vol% YSZ composite cathode.

## 4 Results and Discussion

Simulations comparing experimental results for the 60 vol% LSM, 40 vol% YSZ composite cathode experiments were performed. The simulation parameters were 60 vol% LSM, 40 vol% YSZ, 10% porosity, 945°C, 15 $\mu\text{m}$  thickness and 1 $\mu\text{m}$  particle size. These results are shown in Figure 4.

It was found that the experimental and model prediction followed generally the same trend, but the model predicted much better performance than what was achieved experimentally. A second simulation was performed after decreasing the magnitude of the TPB line length by an order of magnitude (Equation 13). This showed good agreement at lower overpotentials, but the model started to diverge from the experimental data at higher overpotentials. At high overpotentials we would expect concentration overpotential to dominate. The divergence of theoretical and experimental data could suggest that the effective diffusivity is too high or that the electrochemical dependence on species concentrations (reaction order) is too low. Further investigation is re-

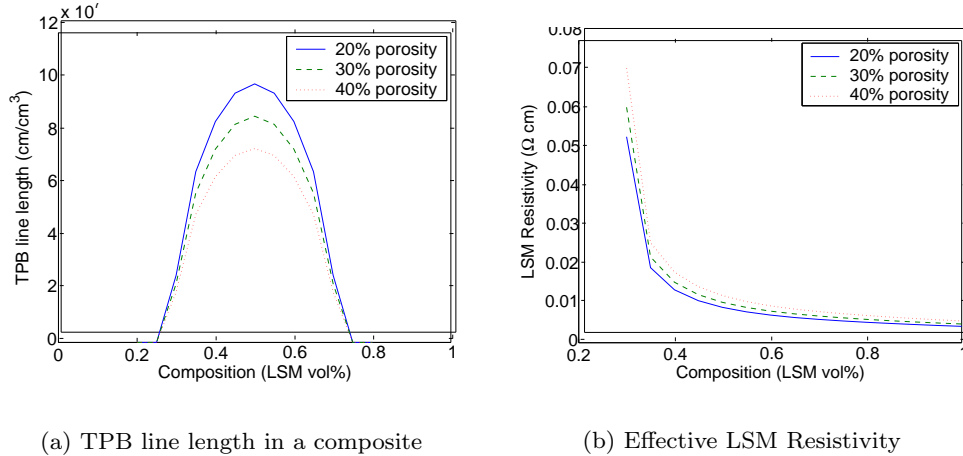


Figure 5: Effect of composition and porosity on the TPB line length and effective LSM resistivity.

quired to determine the cause of this divergence at higher overpotentials.

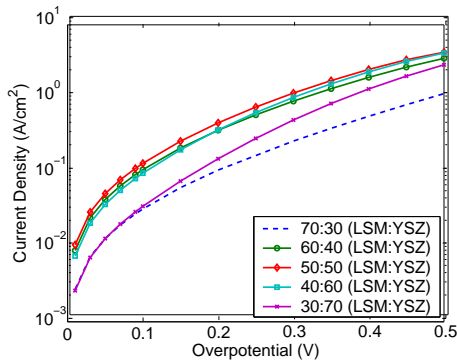
Two major influences on the performance of a composite cathode are its composition (volume fraction of electronically and ionically conducting phases) and its porosity. Both the composition and the porosity will have effects on the TPB line length and the electrical conductivity. Figure 5(a) shows the effect of composition and porosity on the TPB line length and was obtained through Equation 13 for a LSM:YSZ particle size of 1:1. Figure 5(b) shows the effect that composition and porosity have on the effective LSM conductivity and was obtained from Equation 19 for a LSM:YSZ particle size of 1:1.

Figure 5(a) shows that the TPB line length is maximized at a composition of 50 vol% LSM and 20% porosity. This is because at this composition, more LSM and YSZ particles are in contact with each other, extending the active area. High porosity decreases the number of contacting particles and therefore reduces the TPB line length. Figure 5(b) shows the effect of composition and porosity on the effective resistivity of the LSM phase. The higher the LSM volume fraction, the higher the probability of percolation for LSM particles and the lower the resistivity. Lower resistivities are found for low porosity electrodes because pore space hinders the transport of electrons and reduces the continuity of the LSM particle network, thereby increasing resistivity.

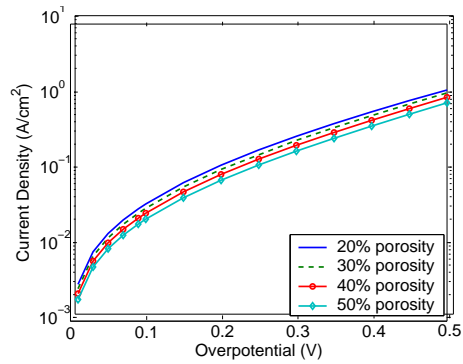
#### 4.1 Parametric Analysis

Simulations of varying composition (70-30 vol% LSM), varying porosity (20-50%) and varying cathode thickness (25, 50, 80, 100 μm) were computed for the 1-dimensional case. A base case of 70 vol% LSM, 30 vol% YSZ, 30% porosity, 100 μm thickness and 1 μm particle sizes was chosen for the parametric study.

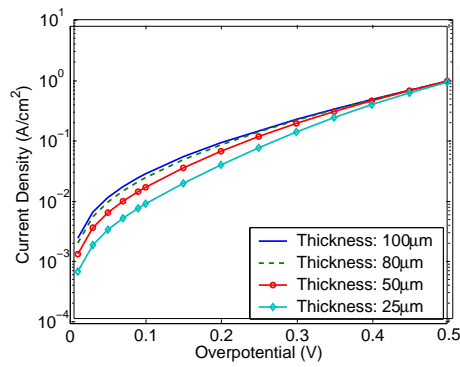
Parametric study results with varying composition, varying porosity and



(a) Varying Composition



(b) Varying Porosity



(c) Varying Thickness

Figure 6: Simulation results of LSM/YSZ composite cathode. Base case: 70 vol% LSM, 30 vol% YSZ, 30% porosity, 100µm thickness.

varying cathode thickness are shown in Figure 6(a), Figure 6(b) and Figure 6(c) respectively. The optimal composition was found to be 50 vol% LSM and 50 vol% YSZ. At this composition, the TPB line length is maximized and therefore the exchange current density of the composite cathode is greatly increased. In addition, both the electronic and ionic conducting phases have good probabilities of percolation. Simulations for a composition of 70 vol% LSM and the 30 vol% LSM reveal that the 30 vol% LSM composition outperforms the 70 vol% LSM composition. This indicates that the ionic conductivity of YSZ is more limiting than the electronic conductivity, since at 30 vol% LSM, the volume fraction of YSZ is large and therefore, so is the effective conductivity due to increased probabilities of percolation for YSZ. Figure 6(b) reveals that the best porosity was found to be 20% porosity. Although a low porosity results in low diffusivities, it also results in higher effective conductivities and higher TPB line lengths. The parametric study also shows that thicker cathodes result in better performance up to a limiting overpotential, at which point each cathode performs equally well. The reasons for this result are not well understood and are currently being investigated.

## 5 Conclusion

A 1-dimensional LSM/YSZ composite cathode micro-model has been developed and electrochemical parameters were obtained experimentally using 3-electrode measurements. Simulation results showed good agreement with experimental data at low overpotential after reducing the calculated TPB line length by an order of magnitude. Parametric analysis from the model showed that 50 vol% LSM, 50 vol% YSZ and 20% porosity is the optimal composite cathode design because of very high TPB line length and a good percolating network of LSM and YSZ phases. More investigation is required for the model predictions regarding thickness of the composite cathode and also the divergence between experimental data and predicted performance at high overpotentials.

## Acknowledgments

Funding for this work has been provided by CAMM and NSERC. The authors are grateful for the help from colleagues at the Fuel Cell Research Centre, Queen's University and the Royal Military College.

## References

- [1] Costamagna, P., Costa, P., and Antonucci, V. (1998) *Electrochimica Acta* **43(3-4)**, 375–394.
- [2] Sunde, S. (2000) *Journal of Electroceramics* **5:2**, 153–182.

- [3] Tanner, C., Fung, K.-Z., and Virkar, A. (1997) *Journal of the Electrochemical Society* **144**, 21–30.
- [4] Chan, S. and Xia, Z. (2001) *Journal of the Electrochemical Society* **148(4)**, A388–A394.
- [5] Chen, X., Chan, S., and Khor, K. (2004) *Electrochimica Acta* **49**, 1851–1861.
- [6] Zhao, F., Armstrong, T., and Virkar, A. (2003) *Journal of the Electrochemical Society* **150(3)**, A249–A256.
- [7] Bouvard, D. and Lange, F. (1991) In *Acta metall. mater.* [9] pp. 3083–3090.
- [8] Sunde, S. (1996) *Journal of the Electrochemical Society* **143(3)**, 1123–1132.
- [9] Chan, S., Chen, X., and Khor, K. (2004) *Journal of the Electrochemical Society* **151(1)**, A164–A172.